British Journal of Pharmacology (2006) 148, 587–598
www.nature.com/bjp

Moclobemide upregulated Bcl-2 expression and induced neural stem cell differentiation into serotoninergic neuron *via* extracellular-regulated kinase pathway

*,[1,2]Shih-Hwa Chiou, [3]Hung-Hai Ku, [4]Tung-Hu Tsai, [1]Heng-Liang Lin, [3]Li-Hsin Chen, [1]Chan-Shiu Chien, [1]Larry L.-T. Ho, [1]Chen-Hsen Lee & *,[5]Yuh-Lih Chang

[1]Department of Medical Research and Education, Taipei Veterans General Hospital and National Yang-Ming University, Taipei, Taiwan; [2]Institute of Clinical Medicine, National Yang-Ming University, Taipei, Taiwan; [3]Institute of Anatomy and Cell Biology, National Yang-Ming University, Taipei, Taiwan; [4]Institute of Traditional Medicine, National Yang-Ming University, Taipei, Taiwan and [5]Department of Pharmacy, Taipei Veterans General Hospital and National Yang-Ming University, Taipei, Taiwan

1 Moclobemide (MB) is an antidepressant drug that selectively and reversibly inhibits monoamine oxidase-A. Recent studies have revealed that antidepressant drugs possess the characters of potent growth-promoting factors for the development of neurogenesis and improve the survival rate of serotonin (5-hydroxytrytamine; 5-HT) neurons. However, whether MB comprises neuroprotection effects or modulates the proliferation of neural stem cells (NSCs) needs to be elucidated.

2 In this study, firstly, we used the MTT (3-(4,5-dimethylthiazol-2-yl)-2,5-diphenyltetrazolium bromide) assay to demonstrate that 50 μM MB can increase the cell viability of NSCs. The result of real-time reverse transcription–polymerase chain reaction (RT–PCR) showed that the induction of MB can upregulate the gene expressions of Bcl-2 and Bcl-xL. By using caspases 8 and 3, ELISA and terminal dUTP nick-end labeling (TUNEL) assay, our data further confirmed that 50 μM MB-treated NSCs can prevent FasL-induced apoptosis.

3 The morphological findings also supported the evidence that MB can facilitate the dendritic development and increase the neurite expansion of NSCs. Moreover, we found that MB treatment increased the expression of Bcl-2 in NSCs through activating the extracellular-regulated kinase (ERK) phosphorylation.

4 By using the triple-staining immunofluorescent study, the percentages of serotonin- and MAP-2-positive cells in the day 7 culture of MB-treated NSCs were significantly increased ($P<0.01$). Furthermore, our data supported that MB treatment increased functional production of serotonin in NSCs *via* the modulation of ERK1/2. In sum, the study results support that MB can upregulate Bcl-2 expression and induce the differentiation of NSCs into serotoninergic neuron *via* ERK pathway.
British Journal of Pharmacology (2006) **148,** 587–598. doi:10.1038/sj.bjp.0706766;
published online 15 May 2006

Keywords: Moclobemide; neural stem cell; Bcl-2; serotonin; ERK; HPLC

Abbreviations: bFGF, fibroblast growth factor-basic; DAPI, 4′,6-diamidino-2-phenylindole; DMEM, Dulbecco's modified Eagle's medium; EGF, epidermal growth factor; ERK, extracellular-regulated kinase; HBSS, Hank's balanced salt solution; 5-HIAA, 5-hydroxyindole acetic acid; HPLC-ECD, high-performance liquid chromatography coupled to electrochemical detection; HVA, homovanillic acid; MB, moclobemide; MTT, 3-(4,5-dimethylthiazol-2-yl)-2,5-diphenyltetrazolium bromide; NCAM, neural cell adhesion membrane protein; NSCs, neural stem cells; PBS, phosphate-buffered saline; RT–PCR, reverse transcription–polymerase chain reaction; TUNEL, terminal dUTP nick-end labeling

Introduction

Depression is one the most common psychiatric disorders, with 10–20% lifetime prevalence (Gurvits *et al*., 1996; Wong & Licinio, 2001). However, the pathophysiology and the underlying mechanisms of depression still remain unclear. Preclinical and clinical findings showed that hippocampal volume in patients with depression is reduced compared to the volume in healthy people (Sapolsky, 1996). MRI imaging studies also showed that hippocampal volume decreases in patients with depression and post-traumatic stress disorder (Sapolsky, 1996; Gurvits *et al*., 1996). Some recent studies have demonstrated that increased cell proliferation and neuron numbers in hippocampus by the administration of antidepressant agents could result in altered behavior in the stress-induced models and patients (File *et al*., 2000; Santarelli *et al*., 2003). These observations suggested that adult hippocampal neurogenesis is decreased by stress and this process of neuron loss may be involved in both the pathogenesis and treatment of mood disorders.

*Authors for correspondence at: Shih-Hwa Chiou, Department of Medical Research and Education, Taipei Veterans General Hospital and National Yang-Ming University, No. 201 Sec. 2 Shih-Pai Road, Shih-Lin, Taipei, Taiwan; E-mail: shchiou@vghtpe.gov.tw or Yuh-Lih Chang, Department of Pharmacy, Taipei Veterans General Hospital, Taipei 112, Taiwan; E-mail: ylchang@vghtpe.gov.tw

Most antidepressant drugs increase the levels of monoamines serotonin (5-hydroxytrytamine; 5-HT) and/or noradrenaline (NA); this suggests that biochemical imbalances within the 5-HT/NA systems may cause the pathogenesis of mood disorders. Moclobemide (MB), an antidepressant drug, which selectively and reversibly inhibit monoamine oxidase-A, could increase the levels of serotonin and norepinephrine. Recent reports have indicated that MB upregulates proliferation of hippocampal progenitor cells in chronically stressed mice (Li *et al*., 2004). Bonnet *et al*. (2000) also showed that the reduction of intracellular pH and neuronal activity of CA3 hippocampal neurons may contribute to the neuroprotective properties of MB. However, whether MB could increase neurogenesis, promote the proliferation of progenitor, and induce specific differentiation in the hippocampus and the central nervous system (CNS) was undetermined.

Neural stem cells (NSCs), derived from hippocampus and other germinal centers of the brain, have been isolated and defined as cells with the capacity of self-renewal and multilineage differentiation (Gage, 2000). NSCs also possess the utilizing potential to develop the transplantation strategies and to screen the candidate agents for neurogenesis in neurodegenerative diseases (Goldman, 2005). With the use of the isolation techniques (Chiou *et al*., 2005), we cultured NSCs derived from the hippocampal tissues of adult rats as a model for the *in vitro* drug–effect test in order to elucidate the role of MB in the cell proliferation and biological effect of NSCs. In addition, the recent studies have shown that the mitogen-activated protein kinase (MAPK)/extracellular-regulated kinase (ERK) signaling pathways may be important for transcriptional activation and protein synthesis of neuronal survival and neuroplasticity in depression (Einat *et al*., 2003; Mercier *et al*., 2004; Hayley *et al*., 2005). The activation of MAPK/ERK pathway can inhibit apoptosis by inducing the phosphorylation of Bad (a proapoptotic protein) and increasing the expression of Bcl-2 (Choi *et al*., 2003; Hayley *et al*., 2005). Moreover, Bcl-2 is also a target for the actions of mood stabilizers and mediates many of beneficial effects of endogenous neurotrophic factors (Segal & Greenberg, 1996; Manji & Chen, 2002). Therefore, we further attempted to investigate the neuroprotection effects and the differentiation capability of MB on NSCs, and to explore the possible mechanisms associated with MAPK/ERK pathway.

Methods

The isolation and culture of NSCs

All animals used were treated in accordance with Animal Care and Use Committee guideline at Taipei Veterans General Hospital. Adult Sprague–Dawley rats (8 weeks old, 250 g) were anesthetized with intraperitoneal phenobarbital (Sigma, St Louis, MO, U.S.A.), and the location of their brains was mapped. Then, the brain was surgically separated from the hippocampus region with the procedure described by Liu *et al*. (2005). Tissues from the hippocampus of adult rats were dissociated and incubated in Hank's balanced salt solution (HBSS) containing collagenase (78 U ml^{-1}) and hyaluronidase (38 U ml^{-1}) for 10 min at 37°C. The tissues were then mechanically dissected and placed in a trypsin solution (1.33 mg ml^{-1}) at 37°C for another 10 min. Dissociated cells were then centrifuged at $150 \times g$ for 5 min. Then the enzyme solution was removed and replaced with serum-free culture media composed of Dulbecco's modified Eagle's medium (DMEM) and F-12 nutrient (1 : 1), including insulin (25 μg ml^{-1}), transferrin (100 μg ml^{-1}), progesterone (20 nM), putrescine (60 μM), sodium selenite (30 nM), and human recombinant epidermal growth factor (EGF) 20 ng ml^{-1}, and fibroblast growth factor-basic (bFGF) 20 ng ml^{-1} (R&D Systems, Minneapolis, MN, U.S.A.). Viable cells were counted by trypan blue exclusion and plated as 5000 cells/200 μl per well in 96-well plates (Corning, Acton, MA, U.S.A.) with no substrate pretreatment (Liu *et al*., 2005).

Chemicals and reagents

The MB was a gift from Roche (Switzerland), the methylenedioxyamphetamine (MDA), serotonin, and 4′,6-diamidino-2-phenylindole (DAPI) were purchased from Sigma-Aldrich (MO, U.S.A.). Liquid chromatographic grade methanol and reagents were obtained from E. Merck (Darmstadt, Germany). Triply deionized water (Millipore, Bedford, MA, U.S.A.) was used for all preparations. The standard stock solution of dopamine (DA) and 5-HT was prepared at a concentration of 10 μg ml^{-1} in a stock solution containing 0.1 M perchloric acid and stored at −70°C in the dark. For the daily preparation of a standard mixture, portions of these stock solutions were thawed at 4°C and diluted to the appropriate concentration with the solution containing 0.1 M perchloric acid.

Cell viability assay

NSCs were seeded on 24-well plates at a density of 2×10^4 cells well^{-1} in medium. The methyl thiazol tetrazolium assay (MTT (3-(4,5-dimethylthiazol-2-yl)-2,5-diphenyltetrazolium bromide) assay; Sigma-Aldrich Co., MO, U.S.A.) was performed for cell viability. NSCs were incubated with 0.25 mg ml^{-1} MTT for 4 h at 37°C and the reaction was terminated by the addition of 100% isopropanol. The amount of MTT fromazon product was determined by using a microplate reader and the absorbance was measured at 560 nm (SpectraMax 250, Molecular Devices, Sunnyvale, CA, U.S.A.). The 0.1% DMSO (Sigma, U.S.A.) was used as a vehicle control in this study.

Real-time reverse transcription–polymerase chain reaction

For real-time reverse transcription–polymerase chain reaction (RT–PCR), the total RNA was extracted using the RNA_{easy} kit (Qiagen, Valencia, CA, U.S.A.) as described by Kao *et al*. (2005). Briefly, total RNA (1 μg) of each sample was reversely transcribed in 20 μl using 0.5 μg of oligo dT and 200 U Superscript II RT (Invitrogen, Carlsbad, CA, U.S.A.). The amplification was carried out in a total volume of 20 μl containing 0.5 μM of each primer, 4 mM $MgCl_2$, 2 μl LightCycler™ – FastStart DNA Master SYBR green I (Roche Molecular Systems, Alameda, CA, U.S.A.), and 2 μl of 1 : 10 diluted cDNA. The quantification in the unknown samples was performed by the LightCycler Relative Quantification Software version 3.3 (Roche Molecular Systems, Alameda, CA, U.S.A.). In each experiment, the GAPDH housekeeping gene was amplified as a reference standard. The primers for

Table 1 Primers for real-time RT–PCR

Gene name		*Primer sequence*	*Location*	*Accession no.*
GADPH	F	GGGCCAAAAGGGTCATCATC	nt 414–434	BC059110.1
	R	ATGACCTTGCCCACAGCCTT	nt 713–733	
Bcl-2	F	GGGATGACTTCTCTCGTCGCTAC	nt 527–550	NM_016993.1
	R	GTTGTCCACCAGGGGTGACAT	nt 721–742	
Bcl-xL	F	CAGCTTCATATAACCCCAGGGAC	nt 402–425	U72350.1
	R	GCTCTAGGTGGTCATTCAGGTAGG	nt 586–610	
Bax	F	GTGGTTGCCCTCTTCTACTTTGC	nt 328–351	NM_017059.1
	R	GAGGACTCCAGCCACAAAGATG	nt 522–544	
Fas	F	AGAGCTGTGGCTACCGGTGAT	nt 301–322	NM_012908.1
	R	AGAGGGATGGACCTTGAGCG	nt 524–544	
MAP2	F	GTTTACATTGTTCAGGACCTCATGG	nt 316–341	U12008.1
	R	TCGGTAAGAAAGCCAGTGTGGT	nt 551–573	
Nestin	F	TGGAGCGGGAGTTAGAGGCT	nt 525–545	NM_012987.1
	R	ACCTCTAAGCGACACTCCCGA	nt 784–805	

F: forward strain; R: reverse strain.

real time RT–PCR are shown as Table 1. PCR reactions were prepared in duplicate and heated to 95°C for 10 min followed by 40 cycles of denaturation at 95°C for 10 s and annealing at 55°C for 5 s; and extension at 72°C for 20 s. All PCR reactions were performed in duplicate. Standard curves (cycle threshold values *versus* template concentration) were prepared for each target gene and for the endogenous reference (GAPDH) in each sample. To confirm the specificity of the PCR reaction, PCR products were electrophoresed on a 1.2% agrose gel.

Enzyme-linked immunosorbent assay (ELISA) and terminal dUTP nick-end labeling (TUNEL) assay

The activities of caspases 8 and 3 were determined by ELISA kit (Medical & Biological Laboratories Co., Ltd, Nagoya, Japan) and quantified by reading at $A_{490\,nm}$ (MRX; Dynatech Laboratories, Chantilly, VA, U.S.A.). Each individual sample was analyzed in triplicate. Furthermore, apoptotic cells were identified by the terminal dUTP nick-end labeling (TUNEL) method (*In situ* Cell Death Detection Kit, POD, Roche Boehringer Mannheim Corp., IN, U.S.A.) as described by Chiou *et al*. (2001). Briefly, the cells with cover slips were washed with 1 × phosphate-buffered saline (PBS), fixed with 4% of paraformaldehyde for 10 min, permeabilized with 0.1% of Triton X-100 for 5 min, and incubated with the TUNEL reagent provided for 1 h. Chromogenic development was then applied with 3-amino-9-ethyl-carbazole, and slides were counterstained with H&E stain.

Immunoblot analysis

After the treatment with MB, the cell lysates of NSCs were collected and the concentration of protein was determined by using the Protein Assay kit (Bio-Rad, Hercules, CA, U.S.A.). Cell extracts with sample buffer were boiled for 5 min and then separated by 10% SDS–PAGE gel. After electrophoresis, the gel was transferred onto a PVDF membrane for immunoblotting. The membrane was first blocked by incubation in nonfat milk at room temperature for 2 h, then incubated with anti-phospho-ERK1/2 (p185/187) antibody (BioSource International Inc., Camarillo, CA, U.S.A.), anti-ERK1/2 and anti-Bcl-2 antibody (Upstate Biotechnology, Waltham, MA, U.S.A.), and anti-actin (Chemicon International, Temecula, CA, U.S.A.) for 2 h at room temperature, washed for five times by Tris-Buffered Saline Tween-20, and then incubated further at room temperature with horseradish peroxidase-conjugated secondary antibody for 2 h. Then, the membrane was washed six times by TBST and specific bands were made visible by chemiluminescence (Santa Cruz Biotechnology, Santa Cruz, CA, U.S.A.).

Immunofluorescence staining

An avidin–biotin complex method was used for the immunohistochemical staining in the differentiated NSCs. Following washes with the 3% hydrogen peroxide and sodium azide, antigenicities were retrieved using a microwave. Each slide was then treated with antibodies for nestin (Chemicon, Temecula, CA, U.S.A.), GFAP (Chemicon, Temecula, CA, U.S.A.), MAP2 (Chemicon, Temecula, CA, U.S.A.), and serotonin (5-HT; polycolonal, Chemicon, Temecula, CA, U.S.A.). Immunoreactive signals were detected with a mixture of biotinylated rabbit anti-mouse IgG and Fluoesave (Calbiochem, La Jolla, CA, U.S.A.).

Chromatographic method for determining neurotransmitters

The sampling technique was constructed according to the design originally described by Cheng *et al*. (2000). The characterization of DA and 5-HT in the effluent and measurement of DA and 5-HT metabolites, that is, DOPAC, homovanillic acid (HVA), and 5-hydroxyindole acetic acid (5-HIAA), in the incubation medium were carried out by the

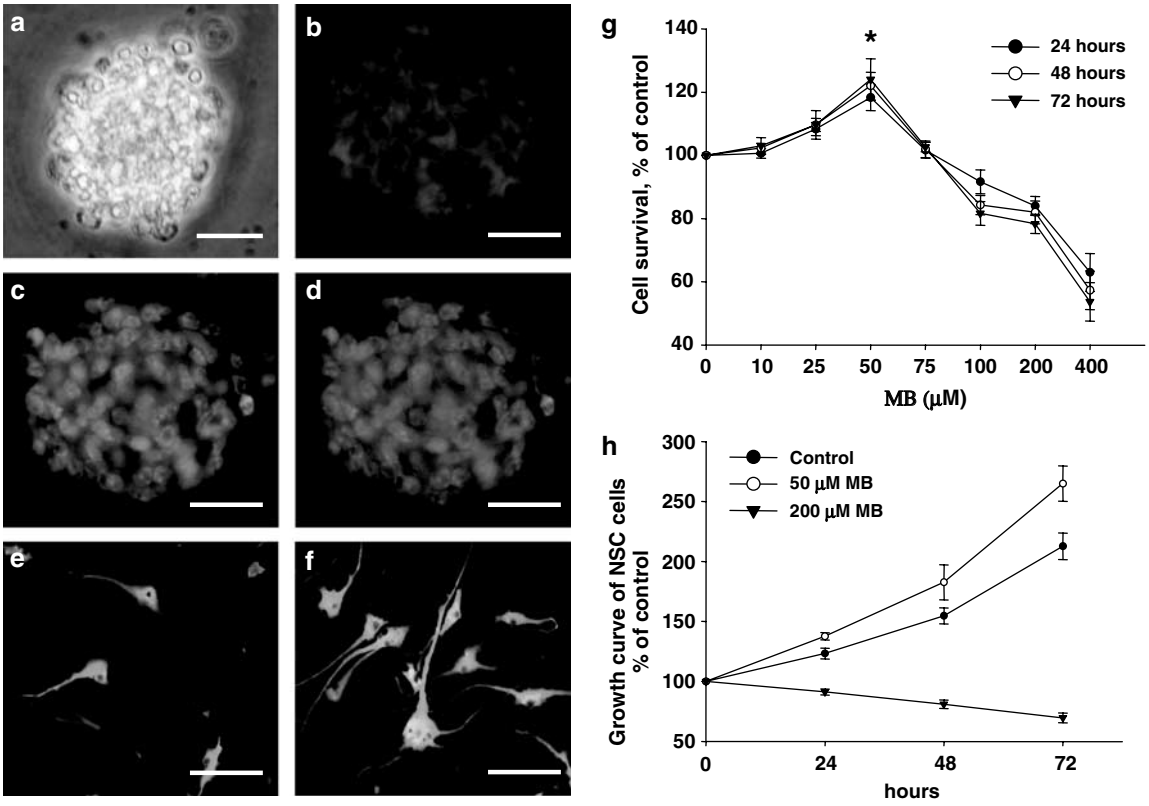

Figure 1 Cultivation of neural stem cells (NSCs) and evaluation of the cell viability in MB-treated NSCs by MTT. (a) NSCs aggregated and formed neurosphere under serum-free medium culture. (b–d) The expressions of nestin (b and d: red fluorescent) and DAPI (c: blue fluorescent; d: merged image) were detected in neurosphere by immunofluorescent assay (bar: 50 μm). (e–f) The GFAP-positive (e: green fluorescent) and MAP-2 positive (green fluorescent) cells were detected in the differentiated NSCs (bar: 20 μm; a–f were performed by three separate experiments). (g) The cell viability of NSCs was analyzed using MTT assay. NSCs were treated with 0, 10, 25, 50, 75, 100, 200, and 400 μM MB for 24, 48, and 72 h. Data (mean $\pm$ s.d. of six separate experiments) are expressed as percentages of the control value (no MB). $^*P<0.05$, as compared to the control. (h) Growth curve of NSC cells: 10^4 NSCs were plated on 6 cm culture dishes with and without MB. After treating with 50 and 200 μM MB for 24, 48, and 72 h, the number of NSCs was counted by hemocytometer, three counts for each point. The 0.1% DMSO was used as a vehicle control.

high-performance liquid chromatography coupled with the electrochemical detection (HPLC-ECD) (Eicom, Kyoto, Japan).

Statistical analysis

Statistical analysis was performed using the ANOVA test. The results were reported as mean $\pm$ s.d. A $P<0.05$ was considered to be statistically significant.

Results

MB modulates the cell viability of NSCs

Tissues from the hippocampus region of rats were dissociated and cultured in DF-12 serum-free medium with bFGF and EGF (20 ng ml^{-1}). After being in culture for 1 week, NSCs aggregated and formed spheroid-like bodies, called neurosphere (Figure 1a). By using the immunofluorescent staining, positive signals of nestin (neural stem cell marker; 94.2 $\pm$ 5.7%; Figure 1b), DAPI (cell nuclei; Figure 1c), and merged imaging (Figure 1d) were detected in neurosphere-like NSCs. To investigate the capacity of multilineage differentiation, the neurosphere-like NSCs were further cultured in the induction medium with a 2% fetal bovine serum (FBS) for 7 days. The percentages of GFAP-positive cells (GFAP: glia marker; 27.7 $\pm$ 5.3%; Figure 1e, green fluorescent) and MAP-2-positive neurons (MAP-2: neuron marker; 34.2 $\pm$ 5.7%; Figure 1f, green fluorescent) were detected in the differentiated NSCs by using the immunofluorescent assay. Nestin, a neural intermediate filament, is expressed at neural crest cells and the early stage of NSCs (Ronald, 1997). Our data revealed that NSCs can aggregate into neurosphere bodies and express high levels of nestin protein under the serum-free medium. Moreover, these NSCs (neurosphere) further exhibited the capacity of the multilineage to differentiate into neurons and astroglia. These features of the NSCs in our study were consistent with the characteristics reported in previous studies (Johansson *et al.*, 1999).

Furthermore, the cell viability and proliferation of NSCs were analyzed using MTT reduction assay. The NSC cells were exposed to 0, 10, 25, 50, 75, 100, 200, and 400 μM concentrations of MB for 24, 48, and 72 h, respectively. As shown in Figure 1g, the cell proliferation increased in the 50 μM MB-treated NSC cells (124.5 $\pm$ 3.8%, $P<0.05$), and the cell viabilities of MB-treated NSCs were significantly decreased when the concentration of MB was greater than 75 μM (Figure 1g and h). When the concentration of MB increased to 400 μM, the viabilities of NSCs significantly decreased in 24 h

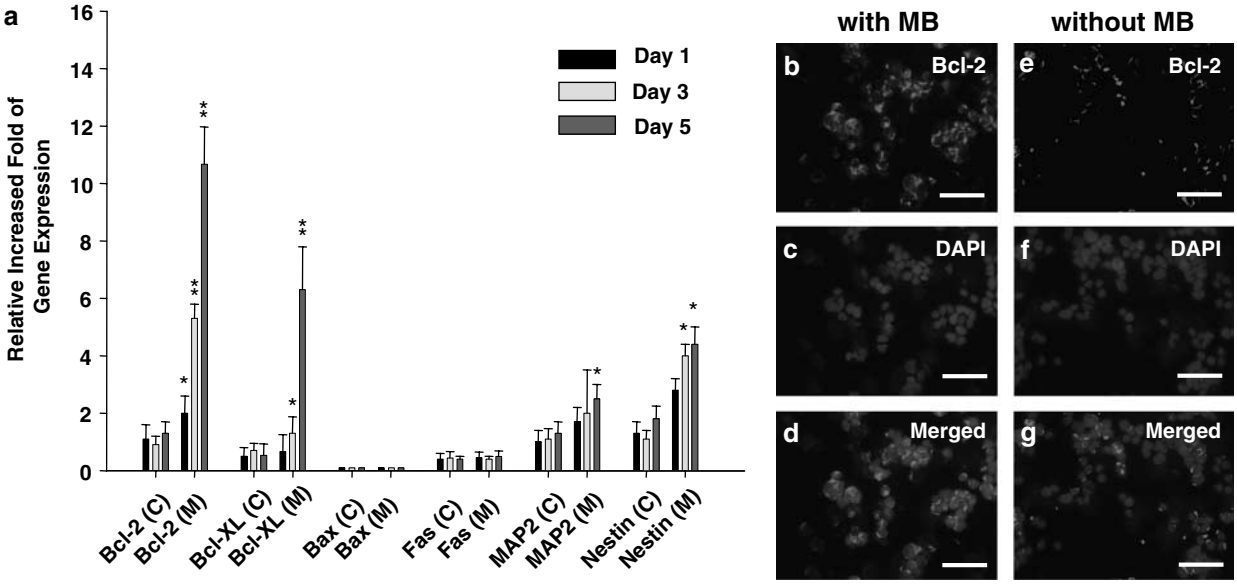

Figure 2 Detection of Bcl-2 expression in MB-treated NSCs by real-time RT–PCR and immunofluorescent assay. (a) The RNA levels of Bcl-2, Bcl-xL, MAP2, and nestin were detected in day-1, -3, -5 MB-treated NSCs by real-time RT–PCR. Data shown here are the mean $\pm$s.d. of three experiments. C: control; M: MB; $^{*}P<0.05$, $^{**}P<0.01$, as compared to the control (no MB). (b–g) By using immunofluorescent assay, the positive signals of Bcl-2 (b, d, e, and g; red fluorescent), DAPI (c, d, f, and g; blue fluorescent), and merged images were identified in MB-treated (b–d) and no MB-treated (e–g) NSCs (bar: 100 μm; b–g were performed by three separate experiments).

(63.1$\pm$5.8%, $P<0.01$), 48 h (56.3$\pm$5.4%, $P<0.01$), and 72 h (52.4$\pm$6.1%, $P<0.01$; Figure 1g). As MB at 50 μM was shown to increase cell survival (Figure 1g and h), the concentration of 50 μM MB was chosen for all further experiments.

Detection of gene expression of MB-treated NSCs by real-time RT–PCR

To further investigate the role of MB in the gene expression of neurosphere-like NSCs, the mRNA expressions of Bcl-2, Bcl-xL, Bax, Fas, MAP2, and nestin were detected in NSCs by real-time RT–PCR (Figure 2a). The result showed that the mRNA levels of Bcl-2 (5.5$\pm$0.4 and 10.6$\pm$1.5 fold, respectively) and Bcl-xL (1.8$\pm$0.3 and 6.3$\pm$1.6 fold, respectively) in the day-3 and day-5 MB-treated NSCs were significantly upregulated compared to NSCs without the MB treatment ($P<0.05$; Figure 2a). In contrast, the expressions of Bax and Fas were not significantly changed both in the MB-treated and in the non-MB-treated NSCs (Figure 2a). The mRNA levels of the MAP2 (2.0$\pm$1.0 and 2.4$\pm$0.3 fold, respectively) and nestin (3.9$\pm$0.4 and 4.4$\pm$0.5 fold, respectively) were slightly increased in the day-3 and day-5 MB-treated NSCs. (Figure 2a). Furthermore, by using the immunofluorescent staining, our data confirmed that the protein expression of Bcl-2 in the day-5 MB-treated NSCs (Figure 2b–d) was significantly increased compared to the NSCs without the treatment of MB (Figure 2e–g).

Detection of the antiapoptotic activity of MB-treated NSCs by ELISA and TUNEL assay

A recent study showed that the NSCs constitutively express the Fas/FasL system and Fas (CD95) receptor on cell membranes, providing a physiological model for the study of the Fas-dependent apoptosis (Semont *et al*., 2004). Consistent with the findings, our real-time RT–PCR results demonstrated that the RNA level of Fas was stably expressed in the day-1, day-3, and day-5 MB-treated NSCs. We further investigated whether the upregulation of Bcl-2 induced by the MB would increase or lessen the Fas-dependent apoptosis in the MB-treated NSCs. The study of FasL-inducing apoptosis (the recombinant protein of FasL, 200 ng ml^{-1}; Upstate Biotechnology; NY, U.S.A.) was conducted and the replicated samples were then added into the MB-treated NSC culture for 48 h. Under the exposed condition of FasL recombinant protein, our data suggested that the apoptotic activities of annexin-5, caspases 8 and 3 in the MB-treated NSCs group were significantly decreased than those in the non-MB-treated group ($P<0.01$; Figure 3a–c). Consistent with the caspases 8 and 3 data, the results of TUNEL assay further suggested that the treatment of MB could protect the FasL-induced apoptosis in the MB-treated NSCs (Figure 3d), but not in the non-MB-treated NSCs (Figure 3d).

Effects of MB on neurite development and neurite expansion

To investigate the roles of MB in the neuronal differentiation of the NSCs, the neuropheres-like NSCs (undifferentiation; Figure 4a) were seeded on the polyornithine-coating plates with 2% FBS. We observed the morphological development (the number of neurite, neurite length, and primary dendrities) of neurons over a period of 7 days in NSCs. As shown in Figure 4b–d, the MB-treated NSCs projected the neurite and differentiated into the dendritic formations with long process. Moreover, the number of neurite, neurite length, and primary

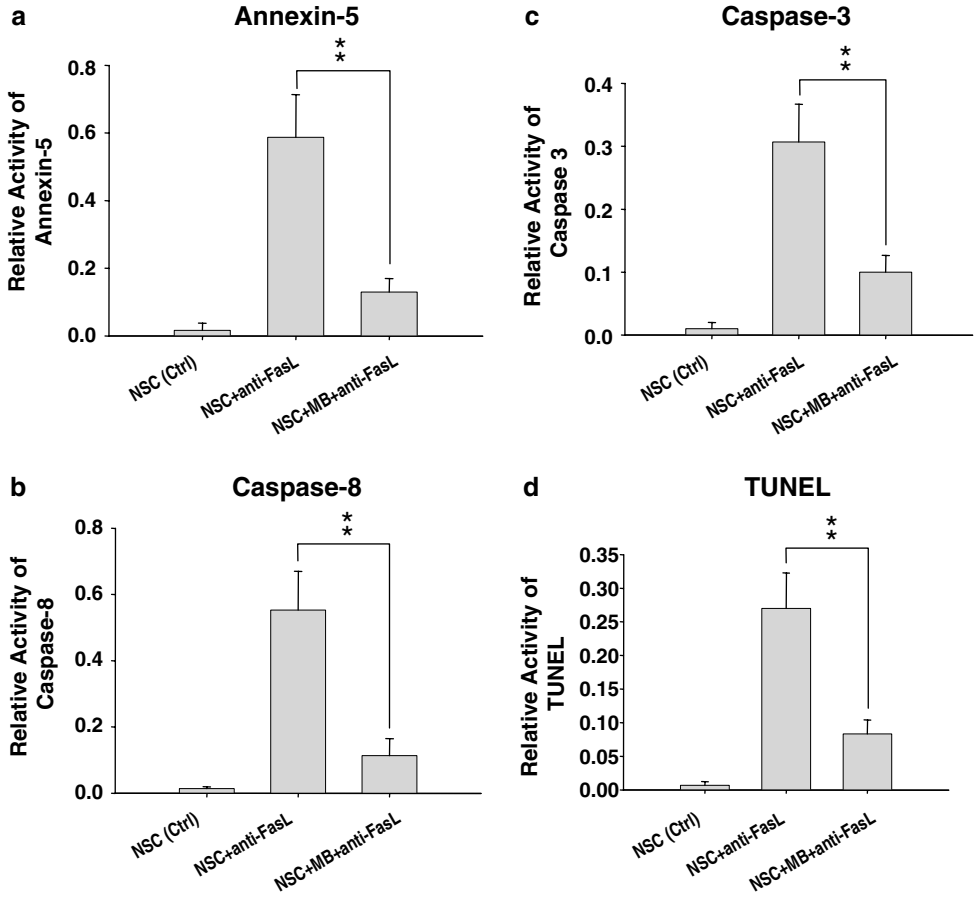

Figure 3 Evaluation of FasL-induced apoptotic activity in NSCs treated with and without moclobemide. (a) The annexin-5 activities were measured in NSCs treated with MB and without MB by using flow cytometry. (b, c) The apoptotic activities of caspase 8 and caspase 3 were detected by ELISA assay. (d) The severity of DNA fragmentation was analyzed by TUNEL assay. The control group (Ctrl: no adding FasL; first column in a–d), the group of NSCs without MB treatment (no MB; second column in a–d), and the group of MB-treated NSCs (third column in a–d). Data shown here are the mean ± s.d. of three experiments; $^{**}P<0.01$.

dendrities in the day-3, day-5, and day-7 MB-treated NSCs were significantly increased than those in the non-MB-treated NSCs ($P<0.05$; Figure 4e–g). To further test whether the MB-stimulated neurite growth is regulated by caspase or MEK signaling pathway, we examined the effects of Z-VAD-FMK (a pan-caspase inhibitor; 40 μM), Z-DEVD-FMK (a selective inhibitor of caspase-3; 40 μM), and PD98059 (MEK inhibitor; 50 μM) on MB-treated and non-MB-treated NSCs. Our data indicated the neurite developments of the NSCs were significantly inhibited by PD98059 ($P<0.01$; Figure 5a and c), but not regulated by Z-VAD-FMK and Z-DEVD-FMK (Figure 5a).

MB upregulates Bcl-2 expression through the phosphorylation of ERK1/2 in NSCs

To determine the biomolecular mechanism of the MB-induced Bcl-2 expression, the protein signal transduction pathway was further explored. After the NSCs were treated with the MB at day 1, day 3, and day 5, the total protein lysate was separated by SDS–PAGE and then detected in terms of antibodies against Bcl-2, phosphorylated ERK 1/2, total ERK 1/2, or internal standard β-actin. The results indicated that MB elevated Bcl-2 protein expression in a time-dependent manner (Figure 6a: no MB treatment; Figure 6b: MB treatment). Concurrently, a higher expression level of phosphorylated ERK 1/2 was detected after the NSCs were treated with the MB for 3 days and 5 days ($P<0.01$; Figure 6b). However, there was no alteration of the total ERK 1/2 expression while the MB incubated with the NSCs (Figure 6b). In order to evaluate whether the activated ERK 1/2 proteins were associated with Bcl-2 upregulation in the MB-treated NSCs, an MAPK/ERK kinase (MEK) inhibitor, PD98059 (Yang *et al*., 2006), was applied (Figure 6c). The results of Western blotting showed that the protein expressions of Bcl-2 and phosphorylated ERK1/2 in the MB-treated NSCs were significantly inhibited by PD98059 (Upper panel, Figure 6c; as compared to only MB treatment, Figure 6b). In contrast, there was no significant change in the total amounts of ERK of the day-1, day-3, and day-5 MB-treated NSCs (Figure 6c).

MB facilitates NSCs differentiation into serotoninergic neurons

To further determine whether MB can promote NSCs being differentiated into serotoninergic neurons, the MB-treated

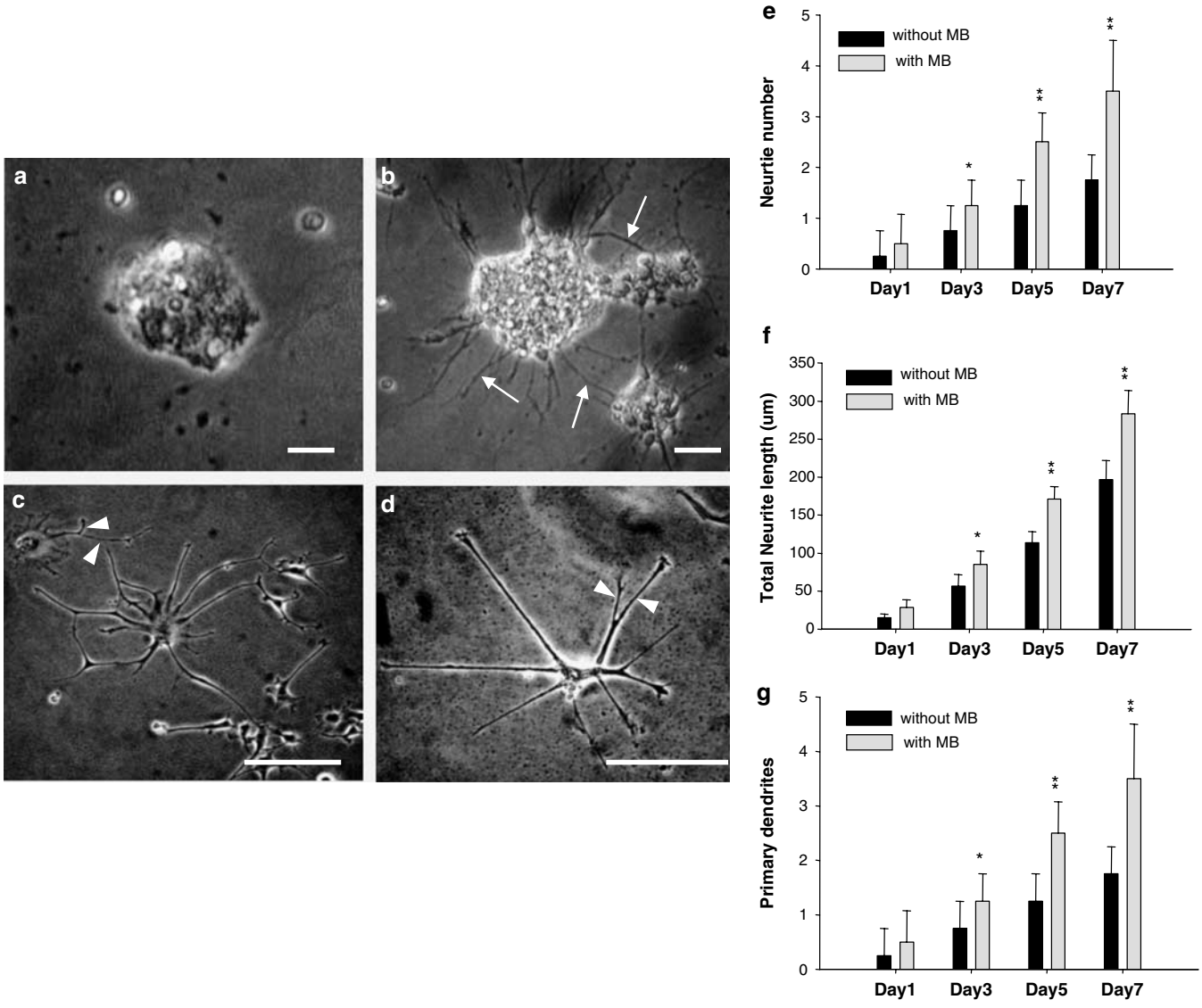

Figure 4 Effects of MB on the neurite development and neurite expansion. (a–d) MB-treated NSCs projected the neurite (arrows) and were differentiated into the dendritic formations with long process (arrowheads: primary branches; bar: 40 μm). The morphological developments of (e) the number of neurite, (f) neurite length, and (g) primary dendrities of the neuronal differentiation were observed and measured in day-1, day-3, day-5, and day-7 cultures of NSCs treated with MB and without MB. Data shown here are the mean $\pm$ s.d. of three experiments; $^{*}P<0.05$; $^{**}P<0.01$, as compared to the control (without MB). The 0.1% DMSO was used as a vehicle control.

NSCs were cultured in the polyornithine-coating plate with 2% FBS. By using triple-staining immunofluorescent assay, the signals of MAP-2 (neuron marker) and 5-HT were detected and colocalized in the same differentiated NSCs (DAPI: nuclei staining; Figure 7a). As shown in Figure 7b–d, the percentages of serotonin- and MAP-2-positive cells in the day-3, day-5, and day-7 cultures of MB-treated NSCs were significantly increased compared to the non-MB-treated NSCs ($P<0.01$). In the day 3, day 5, and day 7 cultures of MB-treated NSCs, PD98059 effectively inhibited the induction rates in both 5-HT-positive cells and MAP2-positive cells ($P<0.05$; Figure 7b–d). Together, our data suggest that MB can facilitate NSCs to differentiate into serotoninergic neurons partly regulated by ERK activation.

Detection of 5-HT concentration released from the MB-treated NSCs by HPLC

To further identify the functional production of 5-HT in these serotoninergic neurons, HPLC was used to measure the concentration of 5-HT in the medium of the MB-treated NSCs (Figure 8). Figure 8a showed a typical chromatogram of a standard mixture (ca. 50 ng ml^{-1} each) containing DOPAC (5.23 min), DA (6.87 min), 5-HIAA (7.78 min), HVA (10.90 min), and 5-HT (15.67 min). Figure 8b and c showed typical chromatograms of HPLC-ECD obtained from the medium only (Figure 8b) and the culture medium from the MB-treated NSCs (Figure 8c). The retention times of 5-HT in Figure 8a and c were identical. The results showed that the 5-HT levels in day 3, day 5, and day 7 of the culture medium

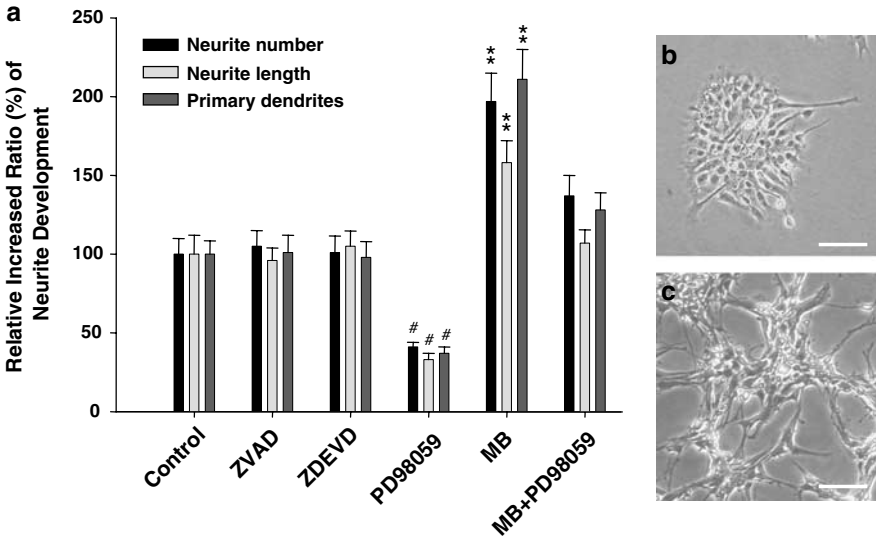

Figure 5 The treatment effects of caspase inhibitors and PD98059 on NSCs with and without MB. (a) The treatment effects of Z-VAD-FMK (a pan-caspase inhibitor), Z-DEVD-FMK (a selective inhibitor of caspase-3), and PD98059 (ERK1/2 inhibitor) on NSCs were examined. Data shown here are the mean ± s.d. of three experiments. Control: no MB treatment. (**$P<0.01$; MB-treated NSCs compared to control group) ($^{\#}P<0.01$; PD98059-treated NSCs compared to control group). (b) The neurite development of differentiated NSCs was specifically inhibited by PD98059. (c) The neuronal formation and neurite expansion in MB-treated NSCs were observed (bar: 30 μm). The 0.1% DMSO was used as a vehicle control.

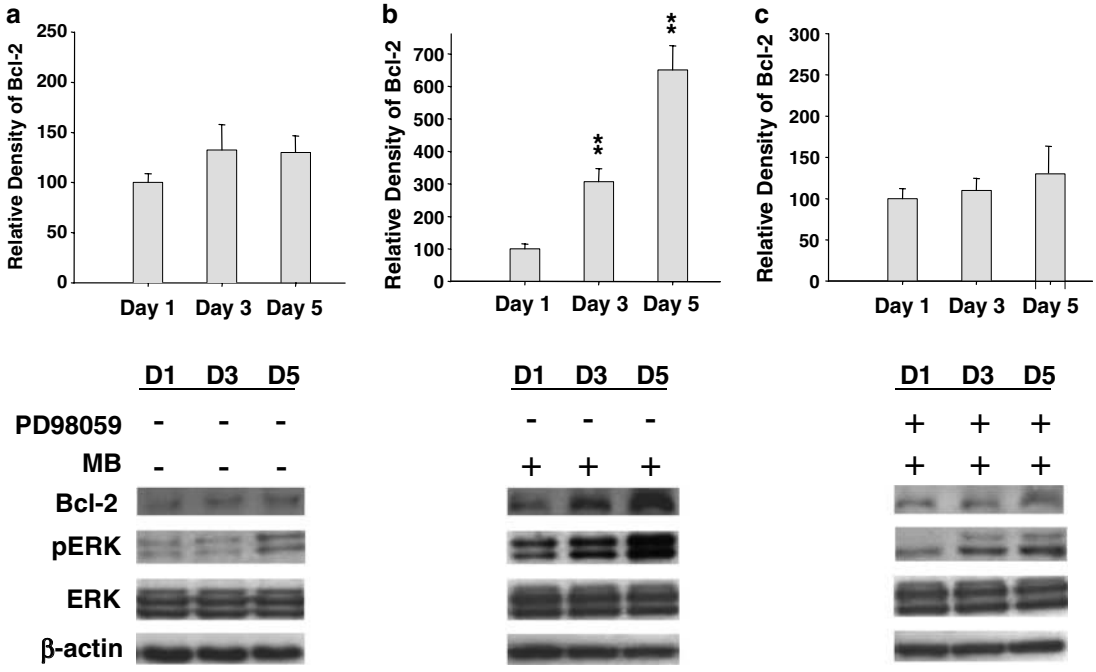

Figure 6 MB upregulated Bcl-2 expression through the phosphorylation of ERK1/2 in NSCs. (a) Detection of the protein amount of Bcl-2, phosphorylated ERK1/2, and total of ERK1/2 in day-1, day-3 and day-5 NSCs without MB treatment by Western blotting assay. (b) The expressions of Bcl-2 and phosphorylated ERK1/2 were upregulated in day-3 and day-5 MB-treated NSCs (no addition of PD98059). (c) The expression levels of Bcl-2 and phosphorylated ERK1/2 in MB-treated NSCs were specifically inhibited by PD98059. Data shown here are the mean ± s.d. of three experiments. **$P<0.01$.

of the MB-treated NSCs were significantly higher than those in the medium without MB-treated NSCs ($P<0.05$; Figure 8d). Furthermore, the productions of 5-HT in the day-3, day-5, and day-7 cultures of MB-treated NSCs were significantly inhibited by PD98059 ($P<0.05$; Figure 8d).

Discussion

The hippocampus has long been associated with learning, memory, and the modulation of emotional responses (Sapolsky, 1997; Eichenbaum, 1999). Previous studies demonstrated that stress-induced atrophy and loss of hippocampal CA3

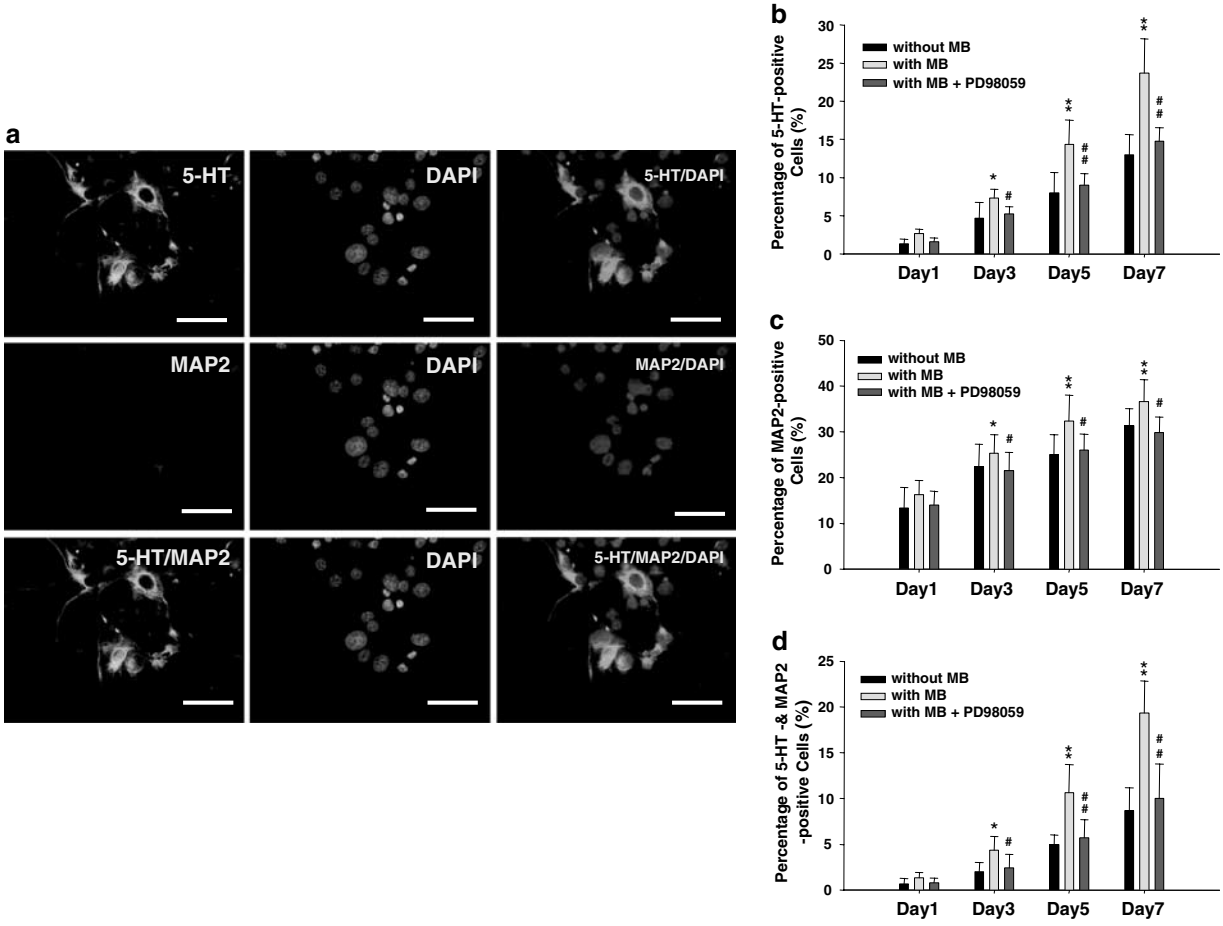

Figure 7 MB promotes NSCs differentiation into serotoninergic neurons. (a) Detection of the protein expression of 5-HT (green fluorescent), MAP2 (red fluorescent), and DAPI (blue fluorescent) in the same differentiated NSCs by using immnunofluorescent assay (bar: 20 μm). The percentages of (b) 5-HT-positive cells, (c) MAP2-positive cells, and (d) both of the 5-HT/MAP2-positive cells in the MB-treated and no MB-treated NSCs were measured by immunofluorescent signals. (b, c) The induction rates of 5-HT-positive cells and MAP2-positive cells in MB-treated NSCs. MB were significantly inhibited by PD98059. Data shown here are the mean $\pm$ s.d. of three experiments. ($^{*}P<0.05$, $^{**}P<0.01$; MB-treated group compared to non-MB-treated group) ($^{\#}P<0.05$, $^{\#\#}P<0.01$; MB- and PD98059-treated group compared to only MB-treated group). The 0.1% DMSO was used as a vehicle control.

pyramidal neurons may contribute to the pathogenesis of depression (Watanabe *et al*., 1992; Duman *et al*., 2000). Recent studies have further suggested that the behavioral effects of chronic use of antidepressant drugs may be mediated by the stimulation of neurogenesis in the hippocampmus of adult rats (Kodama *et al*., 2004). Based on these findings, a novel theory of depression treatment has been proposed; that is, the regulation of neurogenesis in adult brain is a target for the action of antidepressant drugs (Jacobs *et al*., 2000). By using the *in vitro* culture of NSCs from the hippocampus of adult rats, we demonstrated that the 50 μM concentration of MB could increase the viability and proliferation of the NSCs (Figure 1). Our data also confirmed that the 50 μM MB-treated NSC cells can specifically prevent FasL-induced apoptosis in the NSCs through the upregulation of Bcl-2 expression (Figures 2 and 3). The morphological and immunofluorescent observations further revealed that MB not only promotes neuronal axon development (Figures 4 and 5) but also facilitates the differentiation of NSCs toward serotonin-positive neurons (Figure 7).

Studies have shown that the activated ERK1/2 is essential for synaptic plasticity, axon development, neuron differentiation, learning, and memory (Anderson & Tolkovsky, 1999; Impey *et al*., 1999). The elegant study provided by Jiang *et al*. (2005) has shown that cannabinoid can increase proliferation of cultured NSCs derived from the embryonic hippocampal tissues mediated by the activation of ERK1/2 phosphorylation. They further found that cannabinoid treatment promotes neurogenesis in the hippocampal dentate gyrus of adult rats and exerts antidepressant-like effects. Recently, Einat *et al*. (2003) demonstrated that lithium and valproate treatments can significantly increase the protein levels of the phosphor-ERK in the hippocampus of adult rats. Interestingly, our results showed that use of PD98059 (a specific MARK/ERK inhibitor) alone decreased neurite development by approximately 50% compared to control levels (Figure 5). This suggests that neurite development is in part regulated *via* ERK at basal levels, or downstream pathways dependent on ERK activation are implicated. We also demonstrated that the MB treatment increased the induction rate of serotoninergic cells and functional production of serotonin in NSCs, partly *via* the activation of ERK1/2 phosphorylation (Figures 7 and 8). Taken together, these findings indicate that the modulation of ERK signaling pathway by MB plays a critical role in the

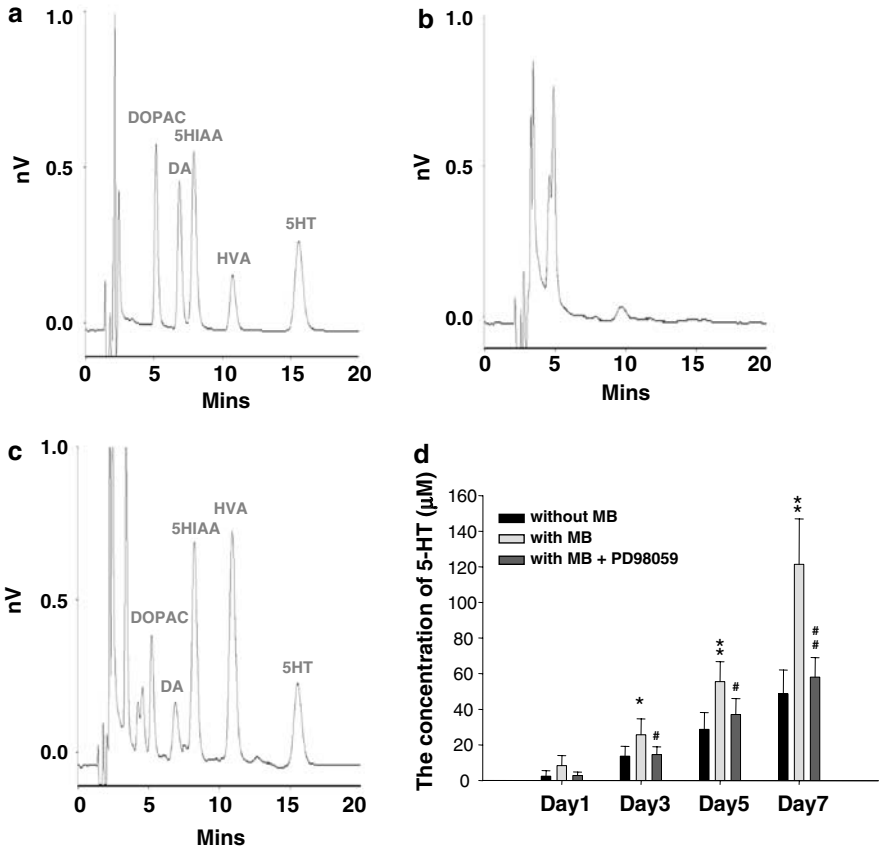

Figure 8 Detection of 5-HT levels in the culture medium of NSCs by HPLC-ECD. Typical chromatograms obtained from (a) a standard mixture containing 3,4-dihydroxyphenylacetic acid (DOPAC; 5.23 min), dopamine (DA; 6.87 min), hydroxyindoleacetic acid (5-HIAA; 7.78 min), homovanillic acid (HVA; 10.90 min), and 5-hydroxytryptamine (5-HT; 15.67 min); analysis was completed within 20 min. (b) A baseline collected from medium only. (c) A sample collected from MB-treated NSC medium. (d) The levels of 5-HT were measured by HPLC-ECD in day 1, day 3, day 5, and day 7 of the culture medium of NSCs treated with MB and no MB. Data shown here are the mean ± s.d. of six experiments. (*$P<0.05$, **$P<0.01$; MB-treated group *via* no MB-treated group) ($^{\#}P<0.05$, $^{\#\#}P<0.01$; MB- and PD98059-treated group *via* only MB-treated group). The 0.1% DMSO was used as a vehicle control.

neurite development, serotoninergic differentiation, and the serotonin production of NSCs.

As for the detailed mechanisms involved in the effects of MB on NSCs, elevated Bcl-2 transcription and translation levels were found in this study. Bcl-2, an antiapoptotic protein, has recently been identified as a neuronal cell death repressor (Garcia *et al*., 1992) and plays an important role in the protection of neural cell death caused by chemical damage and hypoxia (Myers *et al*., 1995). Manakova *et al*. (2005) showed that the Bcl-2 plays a protective role in the oxidative-induced neuronal toxicity and apoptosis in the Parkinson's disease model. As shown in Figure 4, we found that the MB-treated group can protect FasL-induced apoptosis in the NSCs by detection of apoptotic activities. The result of real-time RT–PCR and immunofluorecent study confirmed that the expression levels of Bcl-2 in the MB-treated group were significantly increased compared to those in the control group (Figure 2). In addition, Bcl-2 is also a downstream protein of ERK1/2, which also functions as the responsible kinase for the phosphorylation of Bcl-2 (Tamura *et al*., 2004). A recent study demonstrated that the activation of ERK1/2 could protect against the gastric epithelial cell apoptosis through the maintenance of Bcl-2 expression (Choi *et al*., 2003). Consistent with these findings, our data indicated that MB increased the expression of Bcl-2 in the NSCs through the activation of ERK phosphorylation. Furthermore, the expression of Bcl-2 and the phosphorylation of ERK1/2 were inhibited by PD98059. Thus, the neuroprotection of the MB-treated NSCs could be attributed to the activation of Bcl-2 and the protection of FasL-induced apoptosis in the NSCs *via* ERK pathway.

Furthermore, the gene activation of Bcl-2 helps the neurotransmitter formation, neuroregeneration, and neuroplasticity (Myers *et al*., 1995; Manji *et al*., 2001). Bcl-2 promotes axonal growth and regeneration of the retinal ganglion cells, and its overexpression induces neurite extension and axon regeneration in the midbrain dopaminergic neurons (Chen *et al*., 1997; Daadi *et al*., 2001; Eom *et al*., 2003). Preliminary postmortem brain studies suggest the possible involvement of Bcl-2 in mood disorders, and the upregulation of Bcl-2 will exert trophic effects, and enhance cellular resilience, in the treatment of mood disorders (Manji *et al*., 2001; Bachmann *et al*., 2005). Jiao *et al*. (2005) demonstrated that Bcl-2 enhanced endoplasmic reticulum (ER) calcium signaling through ERK phoshorylation to support the intrinsic regenerative capacity of CNS axons. Hayley *et al*. (2005) further suggested that the reduction of expression levels of Bcl-2 not only decreases the neurogenesis but also impairs the process of neuronal branching under depression and chronic

stressor exposure. Importantly, our data showed that both expression levels of Bcl-2 (Figure 6) and neurite outgrowth (Figure 5) are simultaneously regulated by the ERK pathway, and specifically inhibited by PD98059 (MAPK/ERK inhibitor) in MB-treated NSCs. These observations support that activation of Bcl-2 may participate in the neurite development and prevent stem cell death in MB-treated NSCs through the regulation of MAPK/ERK pathway.

From the therapeutic aspect of the antidepressant treatment, the altered levels of serotonin are closely associated with depression (File *et al*., 2000; Lesch, 2001). Therapeutic interventions for depression increase the serotonergic neurotransmitter, in part by augmenting dentate gyrus neurogenesis and thereby promoting the recovery of depression (Lesch, 2001). In the present study, the functional release of 5-HT (serotonin) from the fluoxetine-treated NSCs were confirmed by the results of HPLC-ECD (Figure 8). In sum, the results of this study support that MB upregulates the Bcl-2 expression and induces the neural stem cell differentiation into serotoninergic neurons *via* the ERK pathway. This *in vitro* model of NSCs can be considered a valuable tool to discover new mechanisms of antidepressant drugs.

This study was supported in part by research grants from the Project (94-365-11 & V95E1-016 & V95E2-007) of Taipei Veterans General Hospital, the Joint Projects of UTVGH (94-P1-08), National Science Council, and Yen-Tjing-Ling Medical Foundation, Taiwan.

References

ANDERSON, C.N. & TOLKOVSKY, A.M. (1999). A role for MAPK/ERK in sympathetic neuron survival: protection against a p53-dependent, JNK-independent induction of apoptosis by cytosine arabinoside. *J. Neurosci.,* **19,** 664–673.

BACHMANN, R.F., SCHLOESSER, R.J., GOULD, T.D. & MANJI, H.K. (2005). Mood stabilizers target cellular plasticity and resilience cascades: implications for the development of novel therapeutics. *Mol. Neurobiol.,* **32,** 173–202 Review.

BONNET, U., LENIGER, T. & WIEMANN, M. (2000). Moclobemide reduces intracellular pH and neuronal activity of CA3 neurones in guinea-pig hippocampal slices – implication for its neuroprotective properties. *Neuropharmacology,* **39,** 2067–2074.

CHEN, D.F., SCHNEIDER, G.E., MARTINOU, J.C. & TONEGAWA, S. (1997). Bcl-2 promotes regeneration of severed axons in mammalian CNS. *Nature,* **385,** 434–439.

CHENG, F.C., KUO, J.S., HUANG, H.M., YANG, D.Y., WU, T.F. & TSAI, T.H. (2000). Determination of catecholamines in pheochromocytoma cell (PC-12) culture medium by microdialysis-microbore liquid chromatography. *J. Chromatogr. A,* **870,** 405–411.

CHIOU, S.H., KAO, C.L., PENG, C.H., CHEN, S.J., TARNG, Y.W., KU, H.H., CHEN, Y.C., SHYR, Y.M., LIU, R.S., HSU, C.J., YANG, D.M., HSU, W.M., KUO, C.D. & LEE, C.H. (2005). A novel *in vitro* retinal differentiation model by co-culturing adult human bone marrow stem cells with retinal pigmented epithelium cells. *Biochem. Biophys. Res. Commun.,* **326,** 578–585.

CHIOU, S.H., LIU, J.H., HSU, W.M., CHEN, S.S., CHANG, S.Y., JUAN, L.J., LIN, J.C., YANG, Y.T., WONG, W.W., LIU, C.Y., LIN, Y.S., LIU, W.T. & WU, C.W. (2001). Up-regulation of Fas ligand expression by human cytomegalovirus immediate-early gene product 2: a novel mechanism in cytomegalovirus-induced apoptosis in human retina. *J. Immunol.,* **167,** 4098–4103.

CHOI, I.J., KIM, J.S., KIM, J.M., JUNG, H.C. & SONG, I.S. (2003). Effect of inhibition of extracellular signal-regulated kinase 1 and 2 pathway on apoptosis and Bcl-2 expression in *Helicobacter pylori*-infected AGS cells. *Infect. Immun.,* **2,** 830–837.

DAADI, M.M., SAPORTA, S., WILLING, A.E., ZIGOVA, T., MCGROGAN, M.P. & SANBERG, P.R. (2001). *In vitro* induction and *in vivo* expression of bcl-2 in the hNT neurons. *Brain Res. Bull.,* **56,** 147–152.

DUMAN, R.S., MALBERG, J., NAKAGAWA, S. & D'SA, C. (2000). Neuronal plasticity and survival in mood disorders. *Biol. Psychiatry.,* **48,** 732–739.

EICHENBAUM, H. (1999). The hippocampus: the shock of the new. *Curr. Biol.,* **9,** R482–R484.

EINAT, H., YUAN, P., GOULD, T.D., LI, J.L., MANJI, H.K. & CHEN, G. (2003). The Role of the extracellular signal-regulated kinase signaling pathway in mood modulation. *J. Neurosci.,* **23,** 7311–7316.

EOM, D.S., CHOI, W.S. & OH, Y.J. (2003). Bcl-2 enhances neurite extension *via* activation of c-Jun N-terminal kinase. *Biochem. Biophys. Res. Commun.,* **314,** 377–381.

FILE, S.E., KENNY, P.J. & CHEETA, S. (2000). The role of the dorsal hippocampal serotonergic and cholinergic systems in the modulation of anxiety. *Pharmacol. Biochem. Behav.,* **66,** 65–72.

GAGE, F.H. (2000). Mammalian neural stem cells. *Science,* **287,** 1433–1438.

GARCIA, I., MARTINOU, I., TSUJIMOTO, Y. & MARTINOU, J.C. (1992). Prevention of programmed cell death of sympathetic neurons by the Bcl-2 prolo-oncogene. *Science,* **258,** 302–304.

GOLDMAN, S. (2005). Stem and progenitor cell-based therapy of the human central nervous system. *Nat. Biotechnol.,* **23,** 862–871.

GURVITS, T.V., SHENTON, M.E., HOKAMA, H., OHTA, H., LASKO, N.B., GILBERTSON, M.W., ORR, S.P., KIKINIS, R., JOLESZ, F.A., MCCARLEY, R.W. & PITMAN, R.K. (1996). Magnetic resonance imaging study of hippocampal volume in chronic, combat-related posttraumatic stress disorder. *Biol. Psychiatry.,* **40,** 1091–1099.

HAYLEY, S., POULTER, M.O., MERALI, Z. & ANISMAN, H. (2005). The pathogenesis of clinical depression: stressor- and cytokine-induced alterations of neuroplasticity. *Neuroscience,* **135,** 659–678.

IMPEY, S., OBRIETAN, K. & STORM, D.R. (1999). Making new connections: role of ERK/MAP kinase signaling in neuronal plasticity. *Neuron,* **23,** 11–14.

JACOBS, B.L., PRAAG, H. & GAGE, F.H. (2000). Adult brain neurogenesis and psychiatry: a novel theory of depression. *Mol. Psychiatry.,* **5,** 262–269.

JIANG, W., ZHANG, Y., XIAO, L., VAN CLEEMPUT, J., JI, S.P., BAI, G. & ZHANG, X. (2005). Cannabinoids promote embryonic and adult hippocampus neurogenesis and produce anxiolytic and antidepressant-like effects. *J. Clin. Invest.,* **115,** 3104–3116.

JIAO, J., HUANG, X., FEIT-LEITHMAN, R.A., NEVE, R.L., SNIDER, W., DARTT, D.A. & CHEN, D.F. (2005). Bcl-2 enhances Ca^{2+} signaling to support the intrinsic regenerative capacity of CNS axons. *EMBO J.,* **24,** 1068–1078.

JOHANSSON, C.B., MOMMA, S. & CLARKE, D.L. (1999). Identification of neural stem cell in the adult mammalian central nervous system. *Cell,* **96,** 389–404.

KAO, C.L., CHIOU, S.H., CHEN, Y.J., SINGH, S., LIN, H.T., LIU, R.S., LO, C.W., YANG, C.C., CHI, C.W., LEE, C.H. & WONG, T.T. (2005). Increased expression of osteopontin gene in atypical teratoid/rhabdoid tumor of the central nervous system. *Mol. Pathol.,* **18,** 769–778.

KODAMA, M., FUJIOKA, T. & DUMAN, R.S. (2004). Chronic olanzapine or fluoxetine administration increases cell proliferation in hippocampus and prefrontal cortex of adult rat. *Biol. Psychiatry.,* **56,** 570–580.

LESCH, K.P. (2001). Serotonergic gene expression and depression: implications for developing novel antidepressants. *J. Affect. Disord.,* **62,** 57–76.

LI, Y.F., ZHANG, Y.Z., LIU, Y.Q., WANG, H.L., YUAN, L. & LUO, Z.P. (2004). Moclobemide up-regulates proliferation of hippocampal progenitor cells in chronically stressed mice. *Acta Pharmacol. Sin.,* **25,** 1408–1412.

LIU, I.H., CHEN, S.J., KU, H.H., KAO, C.L., TSAI, F.T., HSU, W.M., LO, C.W., KUO, Y.H., KUO, C.D., LEE, C.H. & CHIOU, S.H. (2005). Comparison of the proliferation and differentiation ability between adult rat retinal stem cells and cerebral cortex-derived neural stem cells. *Ophthalmologica,* **219,** 171–176.

MANAKOVA, S., SINGH, A., KAARIAINEN, T., TAARI, H., KULKARNI, S.K. & MANNISTO, P.T. (2005). Failure of FK506 (tacrolimus) to alleviate apomorphine-induced circling in rat Parkinson model in spite of some cytoprotective effects in SH-SY5Y dopaminergic cells. *Brain Res.,* **1038,** 83–91.

MANJI, H.K. & CHEN, G. (2002). PKC, MAP kinases and the bcl-2 family of proteins as long-term targets for mood stabilizers. *Mol. Psychiatry,* **7,** S46–S56.

MANJI, H.K., DREVETS, W.C. & CHARNEY, D.S. (2001). The cellular neurobiology of depression. *Nat. Med.,* **7,** 541–547.

MERCIER, G., LENNON, A.M., RENOUF, B., DESSOUROUX, M., COURTN, F. & PIERRE, M. (2004). MAP kinase activation by fluoxetine and its relation to gene expression in cultured rat astrocytes. *J. Mol. Nrurosci.,* **24,** 207–216.

MYERS, K.M., FISKUM, G., LIU, Y., SIMMENS, S.J., BREDESEN, D.E. & MURPHY, A.N. (1995). Bcl-2 protects neural cells from cyanide/aglycemia-induced lipid oxidation, mitochondrial injury, and loss of viability. *J. Neurochem.,* **65,** 2432–2440.

RONALD, M. (1997). Stem cells in the central nervous system. *Science,* **209,** 223–227.

SANTARELLI, L., SAXE, M., GROSS, C., SURGET, A., BATTAGLIA, F., DULAWA, S., WEISSTAUB, N., LEE, J., DUMAN, R., ARANCIO, O., BELZUNG, C. & HEN, R. (2003). Requirement of hippocampal neurogenesis for the behavioral effects of antidepressants. *Science,* **301,** 805–809.

SAPOLSKY, R.M. (1996). Why stress is bad for your brain. *Science,* **273,** 749–750.

SAPOLSKY, R.M. (1997). McEwen-induced modulation of endocrine history: a partial review. *Stress,* **2,** 1–12.

SEGAL, R.A. & GREENBERG, M.E. (1996). Intracellular signaling pathways activated by neurotrophic factors. *Ann. Rev. Neurosci.,* **19,** 463–489.

SEMONT, A., NOWAK, E.B., SILVA LAGES, C., MATHIEU, C., MOUTHON, M.A., MAY, E., ALLEMAND, I., MILLET, P. & BOUSSIN, F.D. (2004). Involvement of p53 and Fas/CD95 in murine neural progenitor cell response to ionizing irradiation. *Oncogene,* **23,** 8497–8508.

TAMURA, Y., SIMIZU, S. & OSADA, H. (2004). The phosphorylation status and anti-apoptotic activity of Bcl-2 are regulated by ERK and protein phosphatase 2A on the mitochondria. *FEBS Lett.,* **569,** 249–255.

WATANABE, Y., GOULD, E. & MCEWEN, B.S. (1992). Stress induces atrophy of apical dendrites of hippocampal CA3 pyramidal neurons. *Brain Res.,* **588,** 341–345.

WONG, M.L. & LICINIO, J. (2001). Research and treatment approaches to depression. *Nat. Rev. Neurosci.,* **2,** 343–351.

YANG, W., CHEN, Y., ZHANG, Y., WANG, X., YANG, N. & ZHU, D. (2006). Extracellular singal-regulated kinases 1/2 mitogen-actived protein kinases pathway is involved in myostatin-regulated differentiation repression. *Cancer Res.,* **66,** 1320–1326.

(Received February 2, 2006
Revised February 28, 2006
Accepted March 2, 2006
Published online 15 May 2006)